Molecular Therapy
Oncolytics
Original Article

A novel vaccinia virus enhances anti-tumor efficacy and promotes a long-term anti-tumor response in a murine model of colorectal cancer

Na Wang,[1] Jiwei Wang,[1] Zhe Zhang,[1] Hua Cao,[2] Wenli Yan,[1] Yongchao Chu,[1] Louisa S. Chard Dunmall,[3] and Yaohe Wang[1,3]

[1]National Centre for International Research in Cell and Gene Therapy, School of Basic Medical Sciences, Academy of Medical Sciences, Zhengzhou University, Zhengzhou 450052, China; [2]ENT Department, The First Affiliated Hospital of Zhengzhou University, Zhengzhou University, Zhengzhou 450052, China; [3]Centre for Biomarkers & Biotherapeutics, Barts Cancer Institute, Queen Mary University of London, London EC1M 6BQ, UK

Colorectal cancer (CRC) is one of the leading causes of mortality and morbidity in the world, and there remains an urgent need to develop long-lasting therapies to treat CRC and prevent recurrence in patients. Oncolytic virus therapy (OVT) has demonstrated remarkable efficacy in a number of different cancer models. Here, we report a novel vaccinia virus (VV)-based OVT for treatment of CRC. The novel VV, based on the recently reported novel VVLΔTKΔN1L virus, was armed with the pleiotropic cytokine interleukin-21 (IL-21) to enhance anti-tumor immune responses stimulated after viral infection of tumor cells. Compared with an unarmed virus, VVLΔTKΔN1L-mIL-21 had a superior anti-tumor efficacy in murine CMT93 subcutaneous CRC models *in vivo*, mediated mainly by $CD8^+$ T cells. Treatment resulted in development of long-term immunity against CMT93 tumor cells, as evidenced by prevention of disease recurrence. These results demonstrate that VVLΔTKΔN1L-mIL-21 is a promising therapeutic agent for treatment of CRC.

INTRODUCTION

Colorectal cancer (CRC) is the third most commonly diagnosed malignancy and the fourth leading cause of cancer death worldwide,[1] with nearly two million new cases and one million fatalities reported in 2018.[2] Recent decades have seen a significant increase in the incidence of CRC, and the global burden of CRC is expected to increase by 60% to more than 2.2 million new cases and 1.1 million deaths by 2030.[3] Common treatments of CRC include local surgical excision, preoperative radiotherapy, extensive surgery for metastatic diseases, palliative chemotherapy, and immunotherapy.[4] These treatments have limited impacts on the cure rate and long-term survival, especially for metastatic patients, and the 5-year survival rate for patients with metastatic CRC remains very poor at approximately 12%.[5,6] Development of new strategies to treat CRC are therefore imperative.

The recent success of cancer immunotherapy has demonstrated the powerful ability of the immune system to detect and eradicate tumors, inspiring scientists to explore new approaches to induce anti-tumor immune responses. Oncolytic virus therapy (OVT) involves the use of tumor-targeted, replication-competent viruses to directly lyse tumor cells and promote a proinflammatory immune environment that supports the development of anti-tumor immune responses.[7] Selective tumor cell killing is a significant advantage of OVT over other traditional therapies, including chemotherapy and radiotherapy, which are highly toxic due to their ubiquitous targeting of replicating cells. Anti-tumor immune responses induced by OVT have direct, targeted efficacy on primary tumors but also induce immune surveillance mechanisms that can clear metastatic tumors and prevent local tumor recurrence.[8] In 2015, the US Food and Drug Administration (FDA) recognized the potential of OVT as a potent therapeutic option and approved the gene-modified oncolytic herpes simplex virus (HSV), Talimogene Laherparepvec (T-VEC), for use in advanced melanoma patients, the first OVT to be approved in the United States.[9]

Vaccinia virus (VV), used extensively during the 1900s as the successful smallpox vaccine, has many features that suggests it as one of the most promising viruses for development of OVT,[10] including a lack of requirement for a specific surface receptor,[11,12] the ability to replicate in hypoxic environments,[13] induction of immunogenic cell death (ICD) pathways,[10] an ability to induce vascular collapse within the tumor microenvironment (TME),[14,15] a large capacity for insertion of exogenous genes, and a long-standing safety profile.[16] Several wild-type and genetically engineered VVs have been tested in preclinical and clinical trials with encouraging results.[10,17] The engineered western reserve (WR) strain of VV with deletions of both thymidine kinase (TK) and vaccinia growth factor genes (known as WRDD) is a commonly used viral strain with strong tumor selectivity and reduced toxicity conferred via the gene deletions but with effective anti-tumor potency in many tumor cell types.[18] We have evaluated the anti-tumor potency and bio-distribution of different VV strains *in vitro* and *in vivo*

Received 17 May 2020; accepted 11 November 2020;
https://doi.org/10.1016/j.omto.2020.11.002.

Correspondence: Yaohe Wang, Centre for Biomarkers & Biotherapeutics, Barts Cancer Institute, Queen Mary University of London, London EC1M 6BQ, UK.
E-mail: yaohe.wang@qmul.ac.uk

and have determined that Lister strain VV demonstrates superior cancer-selective replication in human cancer cell lines and superior antitumor potency using an *in vivo* colon carcinoma model compared to WRDD.[19] For tumor specificity, the TK gene of VV is commonly deleted in VV backbones (named VVLΔTK). TK is required for viral DNA synthesis, rendering the virus replication incompetent in healthy, nondividing cells, where host cell TK is absent, and targeting replication to tumor tissues in which cellular TK, available during host DNA synthesis, can be hijacked by the infecting virus.[20,21] We have recently reported that an additional deletion of the VV 13.8-kDa N1L protein, a neurovirulence factor,[22] can further increase the safety profile of the virus (named VVLΔTKΔN1L) and enhance anti-tumor immune responses, particularly adaptive $CD8^+$ T cell and innate natural killer (NK) cell responses, consequent to viral infection, resulting in superior anti-tumor efficacy of VVLΔTKΔN1L compared to VVLΔTK in a number of *in vivo* murine and hamster models of cancer.[23]

Whereas OVT has shown great potential, research and clinical experience has demonstrated that the use of viral agents alone is insufficient to achieve clinically meaningful responses. Powerful combination therapies are therefore sought, and VV has the necessary capacity for incorporation of transgenes to selectively deliver additional therapeutic agents to the tumor.[24] Interleukin-21 (IL-21) presents as a good candidate for delivery in combination with VV, as it is a potent inducer of T cell activation *in vivo*[25,26] and can inhibit the development of suppressive $Foxp3^+$regulatory T (Treg) cells;[27] induce maturation, activation, and cytolytic potential of natural killer (NK) and NKT (natural killer T) cells;[28,29] promote B cell production of tumor-specific immunoglobulin G (IgG);[30] and inhibit angiogenesis by reducing expression of vascular endothelial growth factor receptor 1 (VEGFR1) and tyrosine kinase with immunoglobulin-like and EGF-like domains 1(TIE1) in endothelial cells.[31] Significantly, there have been no reported adverse effects, even when administered at high doses.[31] Despite its potential, the anti-tumor efficacy of IL-21 as a monotherapy appears limited in early clinical trials.[32] Recently, an oncolytic adenovirus armed with IL-21 (Ad-CCL21-IL-21) demonstrated activity and the induction of tumor-specific cytotoxicity of cytotoxic T lymphocytes (CTLs) to telomerase reverse transcriptase promoter (TERT)-positive tumor cells *in vitro*.[33] Thus, we hypothesized that the potential of IL-21 could be more fully realized by the combination of IL-21 immunotherapy with our virotherapeutic regime.

Here, we demonstrate that VVLΔTKΔN1L, armed with IL-21 (named VVLΔTKΔN1L-mIL-21) is an effective anti-tumor agent using *in vivo* murine models of CRC, inducing robust adaptive T cell responses that can eliminate primary tumors and induce development of anti-tumor immunity to prevent tumor recurrence.

RESULTS

VVLΔTKΔN1L-mIL-21 treatment improves survival in a murine CRC tumor model

VVLΔTKΔN1L-mIL-21 was constructed using CRISPR-Cas9-based homologous recombination to insert the IL-21 gene driven by the H5 promoter into the N1L region of the Lister strain VV genome as recently described.[34,35] To determine the biological characteristics of VVLΔTKΔN1L-mIL-21 *in vitro*, cytotoxicity and replication of the virus were compared to the unarmed virus (VVLΔTKΔN1L-Red Fluorescent Protein (RFP)) in the CRC cell lines CMT93 and CT26. CMT93 cells supported effective replication of VVLΔTKΔN1L-RFP and VVLΔTKΔN1L-mIL-21 (Figure 1A). CT26 cells supported replication of VVLΔTKΔN1L-RFP to high levels, yet the replication of VVLΔTKΔN1L-mIL-21 remains at relatively low levels and peaked at about 40 plaque-forming units (PFUs)/cell at 72 h postinfection (Figure 1A). The cytotoxicity of VVLΔTKΔN1L-mIL-21 was moderately attenuated in CMT93 and CT26 cells compared to VVLΔTKΔN1L-RFP (Figure 1B), but the virus remained competent at cell killing in these cell lines. Additionally, replication and cytotoxicity were tested in a panel of lung tumor cells to determine broader application, and all cell lines examined supported VVLΔTKΔN1L-mIL-21 activity (Figure S1). To assess IL-21 expression by VVLΔTKΔN1L-mIL-21, CMT93 and CT26 cells were infected with virus and the supernatant collected for IL-21 detection by ELISA at 24 h time points postinfection. These data demonstrate effective production of mIL-21 at all time points in both cell lines (Figure 1C). Concentration of IL-21 in the supernatant reached its peak at 48 h (CMT93) or 72 h (CT26) postinfection and subsequently decreased due to its short half-life, as most infected cells were lysed consequent to viral infection.

For analysis of anti-tumor efficacy *in vivo*, CMT93 subcutaneous tumors were established in immunocompetent C57BL/6 mice, and CT26 subcutaneous tumors were established in immunocompetent BALB/c mice. Palpable tumors were injected intratumorally (i.t.) for 6 days (days 1, 3, 5, 7, 9, and 11) using 1×10^8 PFU/injection VVLΔTKΔN1L-mIL-21, VVLΔTKΔN1L-RFP, or PBS, and the tumor growth was monitored. In the CMT93 subcutaneous model, VVLΔTKΔN1L-mIL-21 was significantly more effective at controlling tumor growth and improving survival (Figure 1D) compared to VVLΔTKΔN1L-RFP, and tumors treated with VVLΔTKΔN1L-mIL-21 were cleared in 85.7% (6/7) of animals compared to 42.9% (3/7) of mice treated with VVLΔTKΔN1L-RFP. In the CT26 subcutaneous model, both VVLΔTKΔN1L-RFP and VVLΔTKΔN1L-mIL-21 treatment retarded tumor growth significantly compared with PBS (Figure 1E), although VVLΔTKΔN1L-mIL-21 did not show significant superior antitumor efficacy compared to the control virus.

VVLΔTKΔN1L-mIL-21 treatment modulates the TME and splenic T cell subsets

To determine how VVLΔTKΔN1L-mIL-21 exerts a therapeutic effect, $CD4^+$ and $CD8^+$ T cells infiltrating into CMT93 subcutaneous tumors were examined using immunohistochemistry (IHC). After three i.t. treatments (days 1, 3, and 5), VV coat protein was detected in tumors treated with both VVLΔTKΔN1L-RFP and VVLΔTKΔN1L-mIL-21, and IL-21 was detected after treatment with VVLΔTKΔN1L-mIL-21 (Figure 2A). Both $CD4^+$ and $CD8^+$

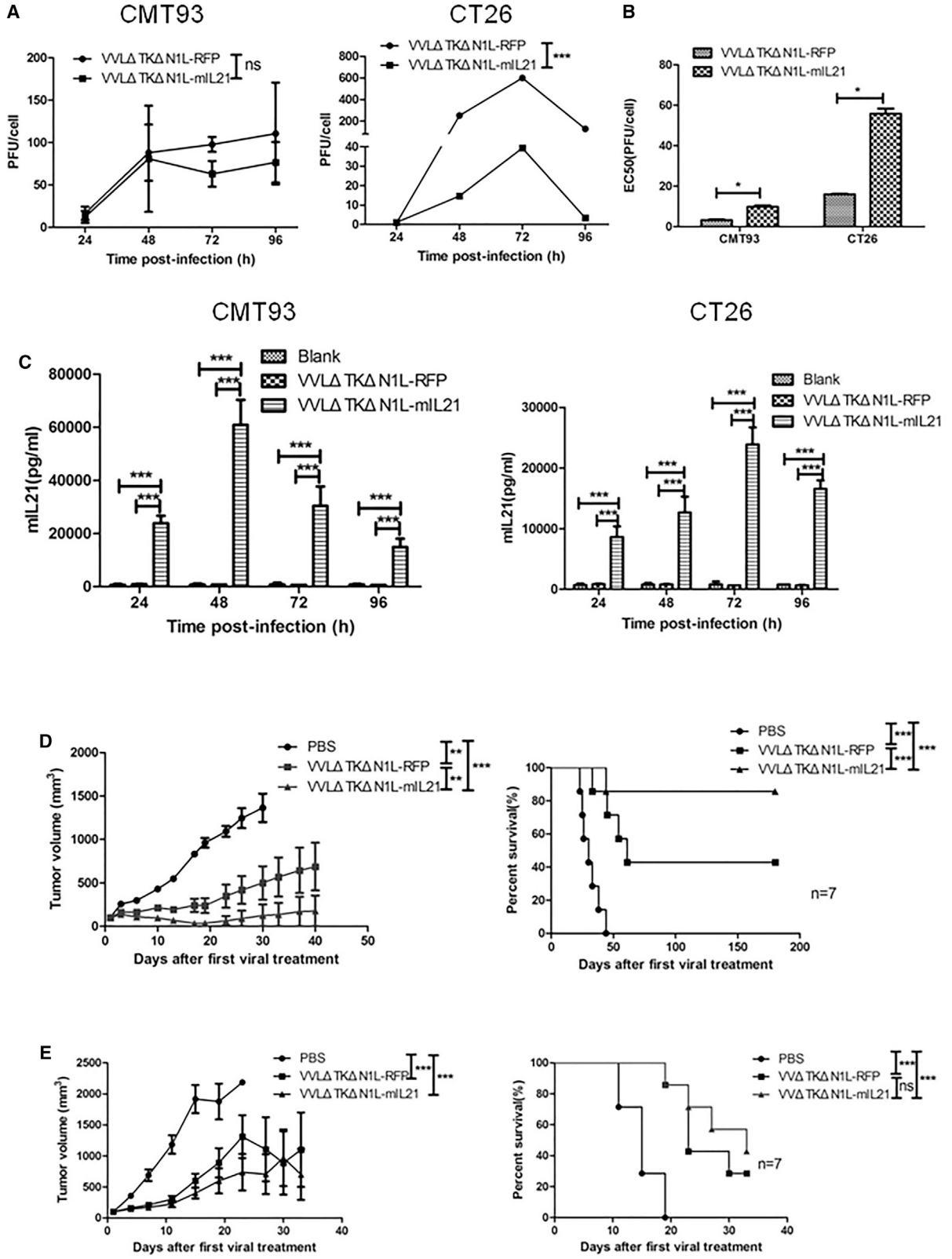

(legend on next page)

T cell infiltrations into tumors were increased after treatment with control or IL-21-armed virus by day 7 (Figures 2A and 2B) and remained elevated 14 and 20 days postinfection (Figures 2C and 2D), although no difference in T cell infiltration was noted between the control and IL-21-expressing virus.

Alterations of T cell subsets in spleens were also examined at each time point following three i.t. injections of the virus. On day 7, after the first viral treatment, total $CD3^+$ T cells from mice spleens treated with VVLΔTKΔN1L-mIL-21 were significantly elevated compared with that from mice treated with VVLΔTKΔN1L-RFP or PBS (Figure 3A). This correlated with an increase in splenic $CD8^+$ T cells on day 7 after VVLΔTKΔN1L-mIL-21 treatment compared to controls (Figure 3B); however, splenic $CD4^+$ T cells were significantly decreased after VVLΔTKΔN1L-mIL-21 treatment compared with VVLΔTKΔN1L-RFP treatment (Figure 3C), possibly reflecting an early mobilization of these cells to tumor sites.

VVLΔTKΔN1L-mIL-21 treatment efficacy relies primarily on $CD8^+$ T cells

To examine in more detail the roles of different immune cells on virus-treatment efficacy of CMT93 subcutaneous tumors, $CD8^+$ T, $CD4^+$ T, or NK cells were depleted by intraperitoneal (i.p.) injection of depletion antibodies and subset depletion confirmed using flow cytometry (Figure S2). Depletion of NK cells had no effect on the treatment efficacy associated with VVLΔTKΔN1L-mIL-21, and $CD4^+$ T cell depletion only modestly affected treatment efficacy (Figure 4). However, depletion of $CD8^+$ T cells had a significantly detrimental effect on the ability of VVLΔTKΔN1L-mIL-21 to control tumor growth (Figure 4), demonstrating that VVLΔTKΔN1L-mIL-21 acts primarily via adaptive $CD8^+$ T cells to mediate anti-tumor effects in this model.

VVLΔTKΔN1L-mIL-21 treatment promotes memory T cell formation and prevents CMT93 tumor recurrence

Central memory T cell subsets ($CD8^+CD44^{hi}CD62L^{hi}$Tcm) in murine spleens were analyzed by flow cytometry after 3 i.t. injections, as above, according to gating criteria for memory T cells (Figure S3). VVLΔTKΔN1L-mIL-21 significantly promoted Tcm-CD8 formation on days 14 and 20 after the first viral treatment (Figure 5A). To determine whether these cells were able to prevent tumor recurrence and thus were indicative of robust anti-tumor effects, 30 days after primary tumors were cleared by OVT, mice were rechallenged with 1×10^7 CMT93 cells (twice the number of cells compared to the primary tumor cell inoculation). At day 1 after rechallenge, the volume of tumor tissues at the inoculation site of some mice reached up to 100 mm^3, due to the injection volume requiring dissipation. Subsequently, the tumor volume gradually decreased to complete disappearance with the absorption of PBS used for inoculation of tumor cells and the activation of anti-tumor immunity that prevented the growth of inoculated cells. Both VVLΔTKΔN1L-RFP- and VVLΔTKΔN1L-mIL-21-treated mice were able to reject CMT93 cells after rechallenge (Figure 5B), but VVLΔTKΔN1L-mIL-21-treated mice were able to reject tumors more rapidly compared to VVLΔTKΔN1L-RFP-treated mice, demonstrating that OVT strategies not only eradicate the primary tumors but also induce long-term antitumor immunity to prevent tumor recurrence. We further examined interferon (IFN)-γ production by splenocytes taken from treated mice. *Ex vivo* stimulation with mitomycin C (MMC)-treated CMT93 cells resulted in significantly increased IFN-γ expression in virus-treated groups compared with that from PBS-treated mice (Figure 5C), with VVLΔTKΔN1L-mIL-21 treatment trending toward more powerful stimulation of anti-tumor immunity. Restimulation with an unrelated cell line, MMC-treated CT26 CRC, was unable to induce IFN-γ expression, demonstrating an induction of specific anti-tumor immunity after virus treatment. Interestingly, only treatment with VVLΔTKΔN1L-mIL-21 was able to significantly induce antiviral immunity in this model. In the context of OVT, antiviral immunity is a double-edged sword. On the one hand, it allows for increased tumor targeting by immune cells that recognize viral antigen on infected tumor cells. On the other hand, this may lead to more rapid viral clearance that reduces the ability of the virus to promote oncolysis. Given the improved efficacy noted *in vivo* using VVLΔTKΔN1L-mIL-21, it may be assumed that in this model, the former consequence has a more powerful effect than the latter, and antiviral immunity may assist in promoting tumor destruction.

DISCUSSION

OVT is widely acknowledged as a validated immunotherapeutic strategy against cancer, with strong potential to act in synergy with other immunotherapies and conventional therapies to improve clinical outcomes via induction of anti-tumor immune responses. VV has many inherent characteristics that make it an ideal oncolytic agent for treatment of pancreatic cancer;[10] however, the limited therapeutic efficacy noted in numerous clinical trials with oncolytic VV suggests that treatment strategies must be optimized to address these limitations, with emphasis placed on improving strategies for overcoming the strongly immunosuppressive TME.[36–38]

We have recently described a novel oncolytic VV, based on the Lister strain backbone that we found to have the most acceptable therapeutic index in comparison to other strains of VV, including the commonly used WR strain, originally reported as the most

Figure 1. Anti-tumor efficacy of VVLΔTKΔN1L-RFP and VVLΔTKΔN1L-mIL-21 in murine subcutaneous CMT93 and CT26 models

(A) Production of infectious vaccinia virus (VV) in CMT93 cells and CT26 cells after infection at an MOI of 5 PFUs/cell. ns, not significant; ***$p < 0.001$. (B) Cytotoxicity of VVLΔTKΔN1L-RFP and VVLΔTKΔN1L-mIL-21 against CMT93 and CT26 cells. *$p < 0.05$. (C) mIL-21 expression by VVLΔTKΔN1L-mIL-21 in CMT93 and CT26 cells. ***$p < 0.001$. (D) CMT93 subcutaneous tumor volumes were decreased after i.t. treatment. **$p < 0.01$, ***$p < 0.001$ (left panel). Kaplan-Meier analysis of treated mice bearing CMT93 tumors was used to determine survival (right panel), n = 7. (E) CT26 subcutaneous tumor volumes were decreased after i.t. treatment. ***$p < 0.001$ (left panel). Kaplan-Meier analysis of treated mice bearing CT26 tumors was used to determine survival (right panel), n = 7.

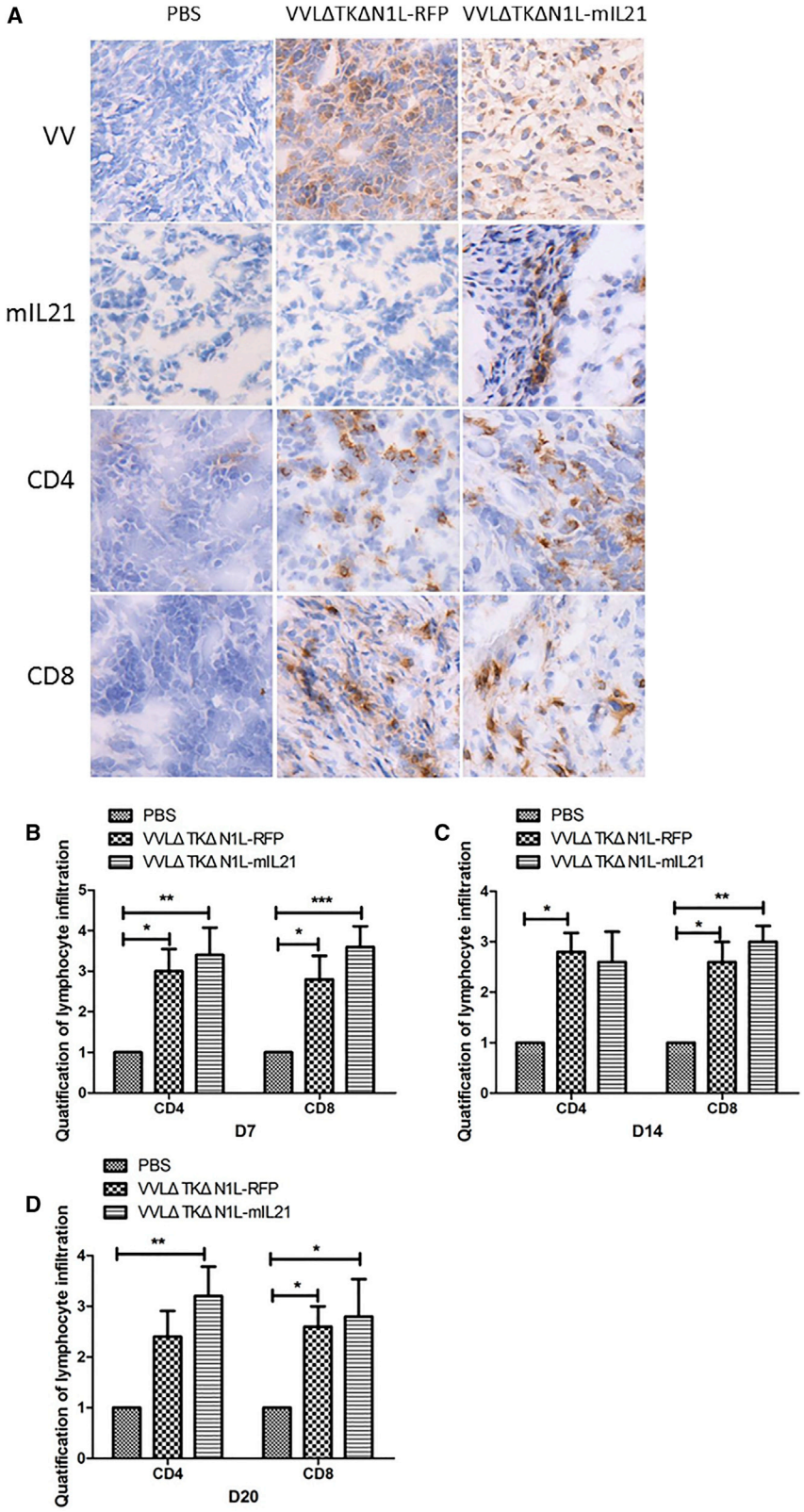

Figure 2. VVLΔTKΔN1L-mIL-21 therapy induces infiltration of T cells into the CMT93 tumor

(A) Representative images of immunohistochemical (IHC) staining for $CD4^+$ T and $CD8^+$ T cells, coat protein of VV, and mIL-21 in CMT93 subcutaneous tumors collected on day 7, n = 3/time point. (B–D) $CD4^+$ T and $CD8^+$ T cells were counted in five high-power fields (HPFs) from each tumor section (×200). Quantitative scores of lymphocyte infiltration within tumors are shown. The scoring was conducted within the subcutaneous tumor on days 7 (B), 14 (C), and 20 (D) after the first viral treatment. The extent of positive cells was categorized into the following four grades: 1, <15 cells/HPF; 2, 16–30 cells/HPF; 3, 31–45 cells/HPF; 4, >45 cells/HPF.

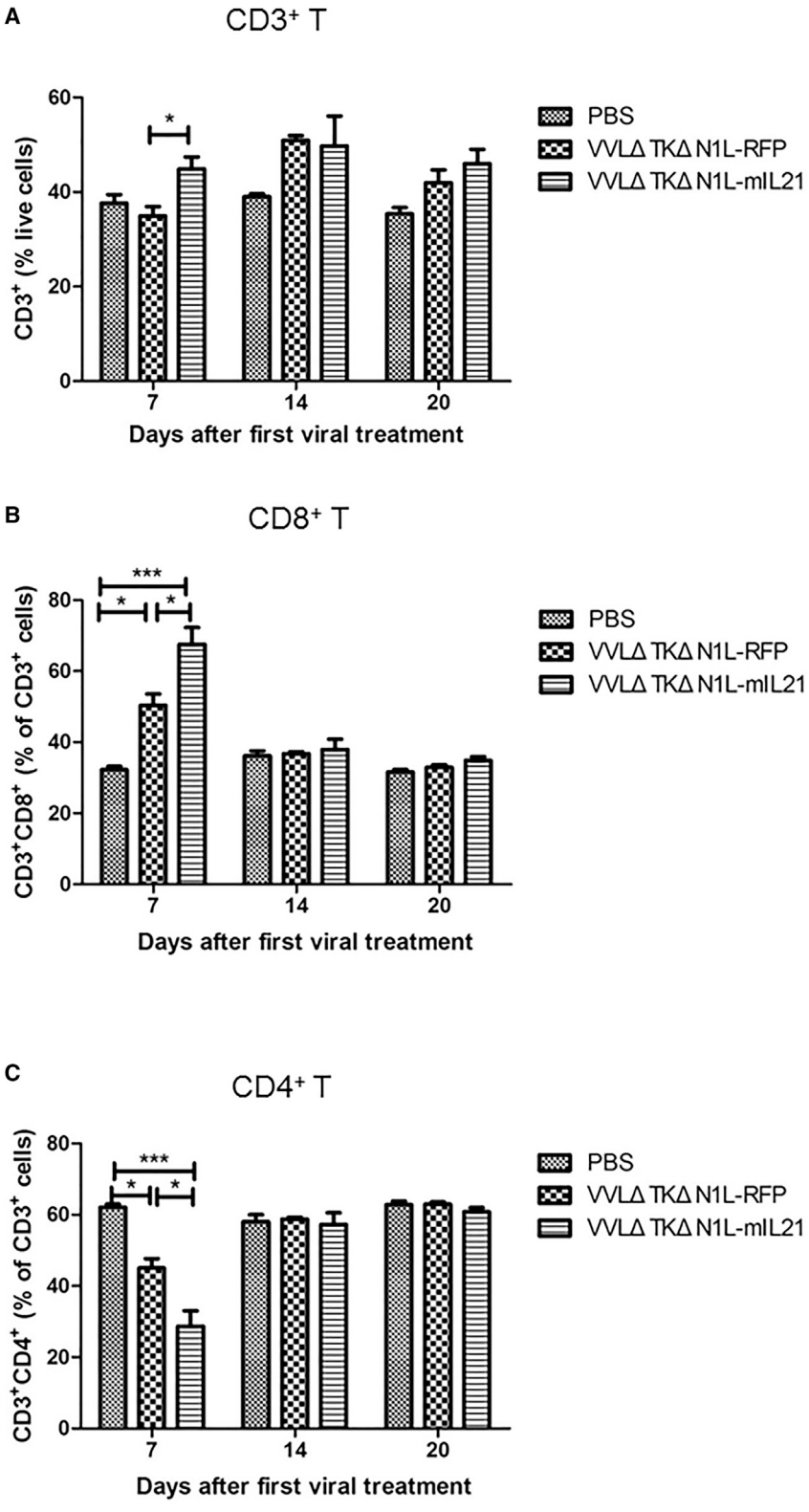

Figure 3. T cell subsets in spleens from VVLΔTKΔN1L-RFP- or VVLΔTKΔN1L-mIL-21-treated mice of the CMT93 subcutaneous model

(A) $CD3^+$ populations as a percentage of live cells in splenocytes of treated mice assessed by gating on $CD3^+$ populations. (B) $CD8^+$ populations as a percentage of live cells in splenocytes of treated mice assessed by gating on $CD3^+CD8^+$ populations. (C) $CD4^+$ populations as a percentage of live cells in splenocytes of treated mice assessed by gating on $CD3^+CD4^+$ populations. *$p < 0.05$, ***$p < 0.001$, n = 3/time point.

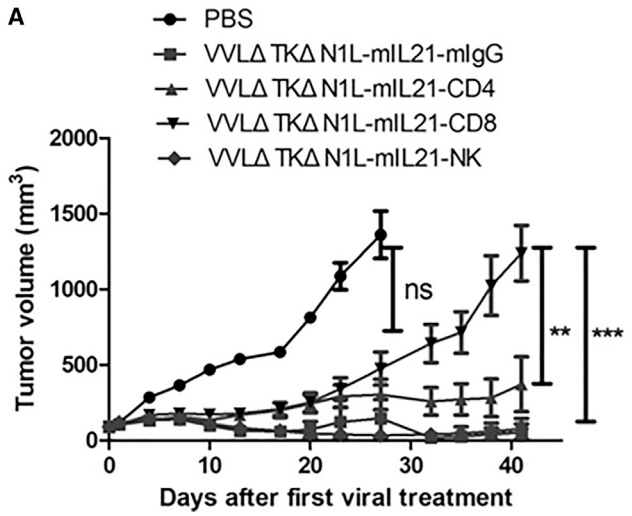

Figure 4. VVLΔTKΔN1L-mIL-21 efficacy is mediated by CD8⁺ T cells in the CMT93 subcutaneous model

CMT93 subcutaneous tumors were established in female C57BL/6 mice and treated as described previously on days 1, 3, 5, 7, 9, and 11. The day before each viral treatment, rat anti-mouse CD4, CD8, NK, or control monoclonal antibodies were injected i.p. n = 7/group. Tumors were measured twice weekly. **p < 0.01, ***p < 0.001.

potent strain of VV.[18,19] Modification of tumor-specific VVL (VVLΔTK, with deletion of the viral *TK* gene) by removing the *N1L* gene (VVLΔTKΔN1L) significantly enhanced both innate and adaptive immune responses systemically and within the TME after i.t. delivery compared to the parental VVLΔTK, resulting in impressive anti-tumor efficacy in murine models of lung and pancreatic cancer.[23]

Here, we report the biological characteristics and anti-tumor efficacy of a novel VV armed with IL-21, VVLΔTKΔN1L-mIL-21, on CRC. Despite the increase of therapeutic options available to improve prognosis for CRC patients, it remains one of the most commonly diagnosed cancers, responsible for up to 10% of all cancer deaths yearly. CMT93 cells, a murine CRC cell line, have a relatively low intrinsic immunogenicity[39] and as such, are not easily controlled by the immune system. However, it has recently been demonstrated that infection with the oncolytic adenovirus could induce ICD pathways in CMT93 cells, and we have shown that VV is able to induce ICD in other tumor cell lines; thus, OVT represents a promising mechanism by which to evoke immune responses against poorly immunogenic tumors.[40,41] Indeed, previous studies have demonstrated sensitivity of colorectal tumor-initiating cells (TICs) to JX-594, the most clinically advanced oncolytic VV—a significant finding, as TICs are generally resistant to standard therapeutic interventions.[42] Here, we demonstrated that whereas VVLΔTKΔN1L-RFP was able to exert anti-tumor efficacy in the CMT93 cancer model, arming the virus with IL-21 significantly enhanced this ability and improved long-term survival of animals. Both viruses were able to induce $CD8^+$ and $CD4^+$ T cell infiltration into the tumor, but the IL-21-armed virus was able to significantly enhance effector $CD8^+$ T cell populations within the spleen, suggesting that IL-21 promotes a higher production of anti-tumor effector $CD8^+$ T cells. Indeed, depletion of $CD8^+$ T cells, but not $CD4^+$ T cells or NK cells, prevented the anti-tumor effect associated with i.t. treatment using VVLΔTKΔN1L-mIL-21. Rechallenge experiments also demonstrated that both viruses were able to evoke long-term immunity against CMT93 tumor cells and prevent tumor recurrence, although addition of IL-21 to the initial treatment resulted in a more rapid clearance of secondary tumors.

We also tested the treatment efficacy of VVLΔTKΔN1L-RFP and VVLΔTKΔN1L-mIL-21 on the CT26 subcutaneous model; both viruses' treatment could retard the tumor growth, yet the treatment efficacy on CT26 models is largely worse than that on CMT93 models. The viral therapeutic efficacy of the virus depends partly on the virus itself, VVLΔTKΔN1L-mIL-21 replication is significantly reduced, with less potency in CT26 cells compared to the control virus (Figures 1A and 1B). This may explain the efficacy result *in vivo* (Figure 1E). In addition, the different genetic backgrounds of CT26 BALB/c mice (T helper [Th]2 dominant) and CMT93 C57BL/6 mice (Th1 dominant) may also affect the immunotherapeutic efficacy of the viruses. Tumor heterogeneity is one important factor affecting the efficacy of tumor therapy, so it is particularly important to advocate personalized tumor therapy. All of these warrant further investigations.

Together, these results describe a rationally constructed OV-based therapeutic platform for CRC that effectively addresses many of the shortfalls of current OV-based platforms in clinical development and may expand the therapeutic landscape for CRC patients.

MATERIALS AND METHODS

Viruses

VVLΔTKΔN1L-RFP was described previously.[43,44] VVLΔTKΔN1L-IL-21 (containing the mouse interleukin-21, named as VVLΔTKΔN1L-mIL-21e) construction was described previously.[34]

Cell lines

All tumor cell lines were obtained from CRUK, Clare Hall, Herts, UK. CV1 cells derived from African monkey kidney were obtained from the American Type Culture Collection (ATCC). CMT93, CV1, LLC, CMT64, CMT167, and CMT170 cells were maintained in Dulbecco's modified Eagle's medium (DMEM) with 10% fetal bovine serum (FBS). CT26 cells were maintained in Roswell Park Memorial Institute (RMPI) 1640 with 10% FBS.

Cytotoxicity assay

VV was first diluted to a multiplicity of infection (MOI) of 1,000 PFUs/cell as initial concentration and then 1:10 serial dilutions used to infect each column of a 96-well plate to a final concentration of 10^{-5} PFUs/cell. Tumor cells were seeded at 2×10^3 cells per well in 96-well plates and separately infected with viruses 16–18 h later. Cell survival on day 6 after viral infection was determined

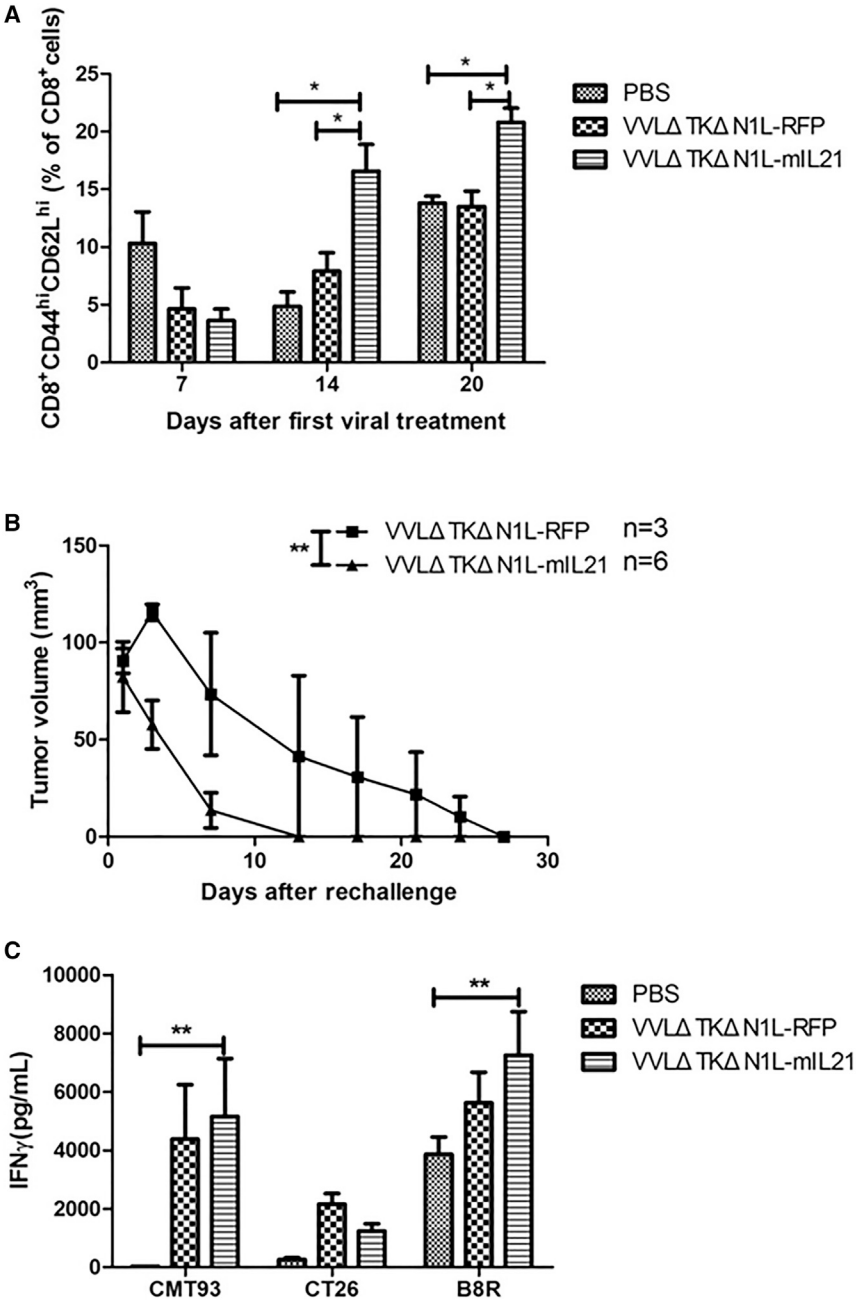

Figure 5. VVLΔTKΔN1L-mIL-21 promotes memory T cell formation and prevents tumor recurrence in the CMT93 subcutaneous model

(A) $CD8^+$ Tcm populations as a percentage of $CD8^+$ cells in splenocytes of treated mice were determined using FACS analysis (n = 9/group). *p < 0.05. (B) Mice that had cleared tumors after i.t. treatment with VVLΔTKΔN1L-RFP or VVLΔTKΔN1L-mIL-21 during efficacy experiments were rechallenged 4 weeks later in the opposite flank with 1×10^7 CMT93 cells and tumor growth measured as done previously. VVLΔTKΔN1L-RFP (n = 3); VVLΔTKΔN1L-mIL-21 (n = 6). **p < 0.01. (C) Splenocytes from treated mice on day 20 after first viral treatment were incubated for 72 h with MMC-treated CMT93 or MMC-treated CT26, and IFN-γ production in response to stimulation was measured by ELISA. **p < 0.01.

by 3-(4,5-dimethylthiazol-2-yl)-5-(3-carboxymethoxyphenyl)-2-(4-sulfophenyl)- 2H-tetrazolium(MTS) assay (Promega), according to the manufacturer's instructions, and EC_{50} values (viral dose killing 50% of tumor cells) were calculated as previously described.[45] All assays were performed at least three times.

Viral replication assay

Tumor cells were seeded at 2×10^5 cells per well in three wells of 6-well plates in medium with 10% FBS, and infected with 5 PFUs/cell of VVLΔTKΔN1L-mIL-21 or VVLΔTKΔN1L-RFP in media with 2% FBS 16–18 h later. Samples were collected at 24-h intervals up to 96 h after infection, freeze thawed three times, and titrated on CV1 cells to determine the 50% tissue culture infective dose (TCID50), as previously described.[46]

In vivo animal studies

All animal studies carried out were approved by the Animal Welfare and Research Ethics Committee of Zhengzhou University (Zhengzhou, China).

Treatment efficacy experiments

5×10^6 CMT93 or CT26 cells were implanted subcutaneously into the right flank of female, 5- to 6-week-old C57BL/6 or BALB/c (for CT26 models) mice. When tumors reached 100 mm^3, mice were divided into 3 groups by matched tumor size to receive six i.t. injections of 1×10^8 PFU/100 μL VVLΔTKΔN1L-mIL-21 or VVLΔTKΔN1L-RFP for treatment or 100 μL PBS for control. Solutions were injected slowly into established tumors to allow injected solution to dissipate evenly during the injection process. Tumor growth was measured using electronic calipers until tumors reached 1.44 cm^2 (w × l) and the area plotted using the following formula:

$$Tumor\ Volume = \frac{\pi w^2 l}{6},$$

where w is width, and l is length.

Tumor growth curves were terminated upon the death of the first animal in each group. Kaplan-Meier survival plots generated that the

experimental animals were recorded as death when the tumor volume reached 1,500 mm^3.

Mechanism experiments

5×10^6 CMT93 cells were implanted subcutaneously into the right flank of female, 5- to 6-week-old C57BL/6 mice. When tumors reached 150 mm^3, mice were randomly divided into three groups by matched tumor size to receive i.t. injections of 1×10^8 PFU/100 μLVVLΔTKΔN1L-mIL-21 or VVLΔTKΔN1L-RFP for treatment or PBS for control on days 1, 3, and 5. On days 7, 14, and 20, subcutaneous tumors, spleens, and lymph nodes were collected from three mice in each group for further investigation, including immunohistochemistry (IHC), fluorescence-activated cell sorting (FACS) analysis, and IFN-γ release assay.

IHC

CMT93 subcutaneous tumors were collected, snap frozen, and stored at −80°C. Frozen tissue was processed for IHC analysis of VV coat protein (1:50 rabbit anti-VV coat protein polyclonal antibody; MorphoSys UK), mIL-21 (Abcam; ab5978) secretion, $CD4^+$ T (BioLegend; 100402), and $CD8^+$ T (BioLegend; 100702) cell infiltration.

IFN-γ release assay

Spleens were collected from a CMT93 subcutaneous mice model and maintained in T cell culture medium (RPMI medium, 10% FBS, 1% penicillin-streptomycin, and 1% sodium pyruvate), and cells were separated using a 70-μm cell strainer. Red blood cells were lysed using red blood cell (RBC) lysis buffer (Sigma-Aldrich) and cells resuspended in complete T cell medium. 5×10^5/well/100 μL splenocytes were seeded into each well of a 96-well plate in triplicate. Cells were restimulated with 5×10^5 MMC-treated CMT93 cells or 5×10^5 MMC-treated CT26 cells. Restimulated splenocytes were incubated for 72 h at 37°C, and the supernatant was collected for ELISA to quantify IFN-γ release.

mIL-21 and IFN-γ ELISA

mIL-21 or IFN-γ protein levels were quantified using IL-21 mouse uncoated ELISA (Invitrogen; 88-8210-88) or mouse IFN-γ uncoated ELISA (Invitrogen; 88-7314-88), according to the manufacturer's instructions. Data (pg/mL) were normalized to the IL-21 standard or IFN-γ standard provided by the kit.

FACS analysis

Spleens from a CMT93 subcutaneous mice model were collected, combined with T cell culture medium, and then pushed through a 70-μm cell strainer to create a single-cell suspension. Cells were centrifuged and the pellet incubated in 5 mL RBC lysis buffer (Sigma-Aldrich). Splenocytes (1×10^6) were prepared and stained with monoclonal antibody (mAb) against mouse CD3 conjugated with phycoerythrin (PE)(eBioscience), mAb against mouse CD4 conjugated with fluorescein isothiocyanate (FITC; eBioscience), mAb against mouse CD8 conjugated with allophycocyanin (APC) (eBioscience), mAb against mouse CD44 conjugated with BV421 (eBioscience), and mAb against mouse CD62L conjugated with PerCP-Cyanine5.5 (eBioscience). Cells were examined using a BD FACSAria III flow cytometer, and data were analyzed using Diva software.

Immune cell subset depletion *in vivo*

5×10^6 CMT93 cells were seeded subcutaneously into 5- to 6-week-old C57BL/6 mice. When tumors reached 100 mm^3, mice were randomly divided into 5 groups by matched tumor size to receive i.t. injections of 1×10^8 PFU/100 μLVVLΔTKΔN1L-mIL-21 twice a week. Depletion mAbs against mouse NK (antibody clone PK136), CD4 (antibody clone GK7.5), CD8 (antibody clone TIB210), and control Ig (mouse anti-KLH mAb) were administered i.p. the day before virotherapy in 200 μL PBS at 200 μg/injection. Injections were continued twice weekly for the duration of the experiment, and FACS analysis was used to confirm depletion. Tumor volumes were measured twice a week as described above. Seven mice per group were used.

Rechallenge of tumor-free animals

The C57BL/6 mice that underwent complete subcutaneous tumor regression following VVLΔTKΔN1L-mIL-21 (n = 6) or VVLΔTKΔN1L-RFP (n = 3) treatment were rechallenged with 1×10^7 CMT93 cells (twice the number of cells compared to the primary tumor cell inoculation) after primary tumors had been cleared for 30 days. Tumor volumes were measured twice weekly.

Statistical analysis

Statistical analysis was performed using GraphPad Prism 5.0. The results were represented as mean ± SD. Comparison between groups was performed using t test, one-way ANOVA, two-way ANOVA, or Kaplan-Meier survival analysis. $p < 0.05$ was considered significant.

SUPPLEMENTAL INFORMATION

Supplemental Information can be found online at https://doi.org/10.1016/j.omto.2020.11.002.

ACKNOWLEDGMENTS

This project was supported by the National Key R&D Program of China (2016YFE0200800), the Nature Sciences Foundation of China (81771776 and U1704282), Pancreatic Cancer UK (2010/YW), and The MRC (MR/M015696/1).

AUTHOR CONTRIBUTIONS

Y.W. conceived and designed the experiments. N.W., J.W., Z.Z., H.C., W.Y., and Y.C. performed the experiments. N.W. and J.W. analyzed the data. N.W. drafted the manuscript. L.S.C.D. and Y.W. interpreted the data and finalized the manuscript.

DECLARATION OF INTERESTS

The authors declare no competing interests.

REFERENCES

1. Buccafusca, G., Proserpio, I., Tralongo, A.C., Rametta Giuliano, S., and Tralongo, P. (2019). Early colorectal cancer: diagnosis, treatment and survivorship care. Crit. Rev. Oncol. Hematol. *136*, 20–30.

2. Bray, F., Ferlay, J., Soerjomataram, I., Siegel, R.L., Torre, L.A., and Jemal, A. (2018). Global cancer statistics 2018: GLOBOCAN estimates of incidence and mortality worldwide for 36 cancers in 185 countries. CA Cancer J. Clin. *68*, 394–424.

3. Arnold, M., Sierra, M.S., Laversanne, M., Soerjomataram, I., Jemal, A., and Bray, F. (2017). Global patterns and trends in colorectal cancer incidence and mortality. Gut *66*, 683–691.

4. Dekker, E., Tanis, P.J., Vleugels, J.L.A., Kasi, P.M., and Wallace, M.B. (2019). Colorectal cancer. Lancet *394*, 1467–1480.

5. Kuipers, E.J., Grady, W.M., Lieberman, D., Seufferlein, T., Sung, J.J., Boelens, P.G., van de Velde, C.J., and Watanabe, T. (2015). Colorectal cancer. Nat. Rev. Dis. Primers *1*, 15065.

6. Siegel, R.L., Miller, K.D., and Jemal, A. (2016). Cancer statistics, 2016. CA Cancer J. Clin. *66*, 7–30.

7. Chiocca, E.A., and Rabkin, S.D. (2014). Oncolytic viruses and their application to cancer immunotherapy. Cancer Immunol. Res. *2*, 295–300.

8. Marelli, G., Howells, A., Lemoine, N.R., and Wang, Y. (2018). Oncolytic Viral Therapy and the Immune System: A Double-Edged Sword Against Cancer. Front. Immunol. *9*, 866.

9. Ott, P.A., and Hodi, F.S. (2016). Talimogene Laherparepvec for the Treatment of Advanced Melanoma. Clin. Cancer Res. *22*, 3127–3131.

10. Guo, Z.S., Lu, B., Guo, Z., Giehl, E., Feist, M., Dai, E., Liu, W., Storkus, W.J., He, Y., Liu, Z., and Bartlett, D.L. (2019). Vaccinia virus-mediated cancer immunotherapy: cancer vaccines and oncolytics. J. Immunother. Cancer *7*, 6.

11. Mercer, J., and Helenius, A. (2008). Vaccinia virus uses macropinocytosis and apoptotic mimicry to enter host cells. Science *320*, 531–535.

12. Moss, B. (2006). Poxvirus entry and membrane fusion. Virology *344*, 48–54.

13. Hiley, C.T., Yuan, M., Lemoine, N.R., and Wang, Y. (2010). Lister strain vaccinia virus, a potential therapeutic vector targeting hypoxic tumours. Gene Ther. *17*, 281–287.

14. Breitbach, C.J., Paterson, J.M., Lemay, C.G., Falls, T.J., McGuire, A., Parato, K.A., Stojdl, D.F., Daneshmand, M., Speth, K., Kirn, D., et al. (2007). Targeted inflammation during oncolytic virus therapy severely compromises tumor blood flow. Mol. Ther. *15*, 1686–1693.

15. Kirn, D.H., Wang, Y., Liang, W., Contag, C.H., and Thorne, S.H. (2008). Enhancing poxvirus oncolytic effects through increased spread and immune evasion. Cancer Res. *68*, 2071–2075.

16. Al Yaghchi, C., Zhang, Z., Alusi, G., Lemoine, N.R., and Wang, Y. (2015). Vaccinia virus, a promising new therapeutic agent for pancreatic cancer. Immunotherapy *7*, 1249–1258.

17. Haddad, D. (2017). Genetically Engineered Vaccinia Viruses As Agents for Cancer Treatment, Imaging, and Transgene Delivery. Front. Oncol. *7*, 96.

18. McCart, J.A., Ward, J.M., Lee, J., Hu, Y., Alexander, H.R., Libutti, S.K., Moss, B., and Bartlett, D.L. (2001). Systemic cancer therapy with a tumor-selective vaccinia virus mutant lacking thymidine kinase and vaccinia growth factor genes. Cancer Res. *61*, 8751–8757.

19. Hughes, J., Wang, P., Alusi, G., Shi, H., Chu, Y., Wang, J., Bhakta, V., McNeish, I., McCart, A., Lemoine, N.R., and Wang, Y. (2015). Lister strain vaccinia virus with thymidine kinase gene deletion is a tractable platform for development of a new generation of oncolytic virus. Gene Ther. *22*, 476–484.

20. Buller, R.M., Smith, G.L., Cremer, K., Notkins, A.L., and Moss, B. (1985). Decreased virulence of recombinant vaccinia virus expression vectors is associated with a thymidine kinase-negative phenotype. Nature *317*, 813–815.

21. Whitman, E.D., Tsung, K., Paxson, J., and Norton, J.A. (1994). In vitro and in vivo kinetics of recombinant vaccinia virus cancer-gene therapy. Surgery *116*, 183–188.

22. Kotwal, G.J., and Moss, B. (1989). Vaccinia virus encodes two proteins that are structurally related to members of the plasma serine protease inhibitor superfamily. J. Virol. *63*, 600–606.

23. Ahmed, J., Chard, L.S., Yuan, M., Wang, J., Howells, A., Li, Y., Li, H., Zhang, Z., Lu, S., Gao, D., et al. (2020). A new oncolytic *Vaccinia virus* augments antitumor immune responses to prevent tumor recurrence and metastasis after surgery. J. Immunother. Cancer *8*, e000415.

24. Sampath, P., and Thorne, S.H. (2013). Arming viruses in multi-mechanistic oncolytic viral therapy: current research and future developments, with emphasis on poxviruses. Oncolytic Virother. *3*, 1–9.

25. Li, Y., Bleakley, M., and Yee, C. (2005). IL-21 influences the frequency, phenotype, and affinity of the antigen-specific CD8 T cell response. J. Immunol. *175*, 2261–2269.

26. Moroz, A., Eppolito, C., Li, Q., Tao, J., Clegg, C.H., and Shrikant, P.A. (2004). IL-21 enhances and sustains CD8+ T cell responses to achieve durable tumor immunity: comparative evaluation of IL-2, IL-15, and IL-21. J. Immunol. *173*, 900–909.

27. Nurieva, R., Yang, X.O., Martinez, G., Zhang, Y., Panopoulos, A.D., Ma, L., Schluns, K., Tian, Q., Watowich, S.S., Jetten, A.M., and Dong, C. (2007). Essential autocrine regulation by IL-21 in the generation of inflammatory T cells. Nature *448*, 480–483.

28. Brady, J., Hayakawa, Y., Smyth, M.J., and Nutt, S.L. (2004). IL-21 induces the functional maturation of murine NK cells. J. Immunol. *172*, 2048–2058.

29. Coquet, J.M., Kyparissoudis, K., Pellicci, D.G., Besra, G., Berzins, S.P., Smyth, M.J., and Godfrey, D.I. (2007). IL-21 is produced by NKT cells and modulates NKT cell activation and cytokine production. J. Immunol. *178*, 2827–2834.

30. Nakano, H., Kishida, T., Asada, H., Shin-Ya, M., Shinomiya, T., Imanishi, J., Shimada, T., Nakai, S., Takeuchi, M., Hisa, Y., and Mazda, O. (2006). Interleukin-21 triggers both cellular and humoral immune responses leading to therapeutic antitumor effects against head and neck squamous cell carcinoma. J. Gene Med. *8*, 90–99.

31. Castermans, K., Tabruyn, S.P., Zeng, R., van Beijnum, J.R., Eppolito, C., Leonard, W.J., Shrikant, P.A., and Griffioen, A.W. (2008). Angiostatic activity of the antitumor cytokine interleukin-21. Blood *112*, 4940–4947.

32. Thompson, J.A., Curti, B.D., Redman, B.G., Bhatia, S., Weber, J.S., Agarwala, S.S., Sievers, E.L., Hughes, S.D., DeVries, T.A., and Hausman, D.F. (2008). Phase I study of recombinant interleukin-21 in patients with metastatic melanoma and renal cell carcinoma. J. Clin. Oncol. *26*, 2034–2039.

33. Li, Y., Li, Y.-F., Si, C.-Z., Zhu, Y.-H., Jin, Y., Zhu, T.-T., Liu, M.-Y., and Liu, G.-Y. (2016). CCL21/IL21-armed oncolytic adenovirus enhances antitumor activity against TERT-positive tumor cells. Virus Res. *220*, 172–178.

34. Yuan, M., Gao, X., Chard, L.S., Ali, Z., Ahmed, J., Li, Y., Liu, P., Lemoine, N.R., and Wang, Y. (2015). A marker-free system for highly efficient construction of vaccinia virus vectors using CRISPR Cas9. Mol. Ther. Methods Clin. Dev. *2*, 15035.

35. Yuan, M., Wang, P., Chard, L.S., Lemoine, N.R., and Wang, Y. (2016). A Simple and Efficient Approach to Construct Mutant Vaccinia Virus Vectors. J. Vis. Exp. *30*, 54171.

36. Achard, C., Surendran, A., Wedge, M.E., Ungerechts, G., Bell, J., and Ilkow, C.S. (2018). Lighting a Fire in the Tumor Microenvironment Using Oncolytic Immunotherapy. EBioMedicine *31*, 17–24.

37. Kaufman, H.L., Kohlhapp, F.J., and Zloza, A. (2015). Oncolytic viruses: a new class of immunotherapy drugs. Nat. Rev. Drug Discov. *14*, 642–662.

38. Raja, J., Ludwig, J.M., Gettinger, S.N., Schalper, K.A., and Kim, H.S. (2018). Oncolytic virus immunotherapy: future prospects for oncology. J. Immunother. Cancer *6*, 140.

39. Chong, H., Todryk, S., Hutchinson, G., Hart, I.R., and Vile, R.G. (1998). Tumour cell expression of B7 costimulatory molecules and interleukin-12 or granulocyte-macrophage colony-stimulating factor induces a local antitumour response and may generate systemic protective immunity. Gene Ther. *5*, 223–232.

40. Yamano, T., Kubo, S., Fukumoto, M., Yano, A., Mawatari-Furukawa, Y., Okamura, H., and Tomita, N. (2016). Whole cell vaccination using immunogenic cell death by an oncolytic adenovirus is effective against a colorectal cancer model. Mol. Ther. Oncolytics *3*, 16031.

41. Lu, S., Zhang, Z., Du, P., Chard, L.S., Yan, W., El Khouri, M., Wang, Z., Zhang, Z., Chu, Y., Gao, D., et al. (2020). A Virus-Infected, Reprogrammed Somatic Cell-Derived Tumor Cell (VIReST) Vaccination Regime Can Prevent Initiation and Progression of Pancreatic Cancer. Clin. Cancer Res. *26*, 465–476.

42. Conrad, S.J., and Essani, K. (2014). Oncoselectivity in Oncolytic Viruses against Colorectal Cancer. J. Cancer Ther. *5*, 1153–1174.

43. Yuan, M., Zhang, W., Wang, J., Al Yaghchi, C., Ahmed, J., Chard, L., Lemoine, N.R., and Wang, Y. (2015). Efficiently editing the vaccinia virus genome by using the CRISPR-Cas9 system. J. Virol. *89*, 5176–5179.

44. Dénes, B., Yu, J., Fodor, N., Takátsy, Z., Fodor, I., and Langridge, W.H. (2006). Suppression of hyperglycemia in NOD mice after inoculation with recombinant vaccinia viruses. Mol. Biotechnol. *34*, 317–327.

45. Wang, Y., Hallden, G., Hill, R., Anand, A., Liu, T.-C., Francis, J., Brooks, G., Lemoine, N., and Kirn, D. (2003). E3 gene manipulations affect oncolytic adenovirus activity in immunocompetent tumor models. Nat. Biotechnol. *21*, 1328–1335.

46. Reed, L.J., and Muench, H. (1938). A simple method of estimating fifty percent end-points. Am. J. Hyg. *27*, 493–497.